

Ultra-high energy Cosmic Rays and the Extragalactic Gamma Ray Flux.

¹A.D. Erlykin ^{a,b} and A.W. Wolfendale ^b

(a) P N Lebedev Physical Institute, Moscow, Russia.

(b) Physics Department, Durham University,
Durham, DH1 3LE, UK

April 8, 2014

Abstract

Ultra-high energy cosmic rays interacting with the radiation fields in the universe cause electromagnetic cascades resulting in a flux of extragalactic gamma rays, detectable to some 100 GeV. Recent precise measurements of the extragalactic gamma ray flux by Fermi-LAT, coupled with estimates of the background from active galactic nuclei of various types, allows limits to be set on the cascade component. By comparison with prediction and, making various assumptions, ie taking a particular model, limits can be set on the maximum energy to which ultra-high energy particles can be accelerated.

If our model is correct, it is unlikely that the maximum energy is above 100 EeV, in turn, the apparent ‘GZK’ cut-off in the measured ultra-high energy spectrum could instead be due to a fall-off in the intrinsic emergent particle spectrum. However, it is not possible to be dogmatic at the present time because of uncertainty in many of the parameters involved. We have used recent estimates of the range of parameters and have found that although our model has parameters in the allowable ranges the uncertainties are so large that our result is not unique, although the method is satisfactory. The result must thus, so far, be taken as an indication only.

1

1 Introduction

Some decades ago [1] it was pointed out that there is a constraint on the energy spectrum of the ultra-high energy cosmic ray (UHECR) intensity caused by the electromagnetic cascade of photons and electrons initiated by the initial interaction of the UHECR with the cosmic microwave background (CMB). Later interactions with both the CMB and

¹Corresponding author: tel +74991358737
E-mail address: erlykin@sci.lebedev.ru

the starlight and infra-red fields cause the cascade to extend down to the MeV gamma ray region.

Comparison of the expected flux for various (proton) production scenarios [2] with the then measured extragalactic (EG) gamma flux [3] allowed limits to be put on the former. With more recent estimates of the EG gamma flux by Fermi-LAT [4] and superior estimates of the contribution from unresolved sources (active galactic nuclei, AGN) [5] an improved production scenario can be derived. Our particular interest is the maximum energy achievable at the sites of acceleration, the analysis being made for both primary protons and iron nuclei. Regarding the mass composition at the highest energies, the case for heavy nuclei was made early on (see, eg, [6]) and recent analysis give some support [7,8,9].

In what follows, we start by assuming that our initial calculations [1,2] were correct and follow them through with the Fermi-LAT gamma ray spectrum [4] to establish the method and arrive at tentative conclusions. This is followed by an examination of the limits that can be put on the various input parameters, and on the consequent result using a recent analysis [9].

Of relevance is the observation by the Pierre Auger Observatory (PAO) that above 55 EeV, some 24% of the particles come from the giant Cen-A radiogalaxy within a direction of 40 degrees [10] to a significance level of 4%. Others [11,12] have developed theories assuming this identification. The relation of this result to the problem in hand will also be examined.

2 The diffuse EG gamma ray spectrum.

Figure 1 shows the Fermi-LAT spectrum [4] in comparison with our earlier estimate [13]. The steeper contemporary spectrum can be understood in terms of a more accurate 'discrete source' correction, the new measurements allowing weaker sources to be identified. The effect of the recent [5] correction for AGN is shown. It will be noted that the EG gamma ray flux available for cascade gamma rays is small, ie of order of the discrete source contribution itself.

3 The cascade gamma ray spectrum.

3.1 Effect of maximum energy and mass.

The cascade calculations referred to in [2] involve determining the energy abstracted from the EG particle beam by the interactions with the CMB, it is this energy that is propagated by way of subsequent interactions with the radiation fields to give a gamma ray spectrum that extends down to the MeV region. The intensity in the GeV region is proportional to the energy abstracted. This latter is derived in a straightforward way from application of the attenuations to the assumed primary (injection) spectrum.

The profile of the attenuation mean free path (λ) versus energy for both protons and iron nuclei has been known for many decades. Using recent calculations [14,15], for protons λ falls from its red-shift value of 4000 Mpc to 1000 Mpc at 10 EeV, 200 Mpc

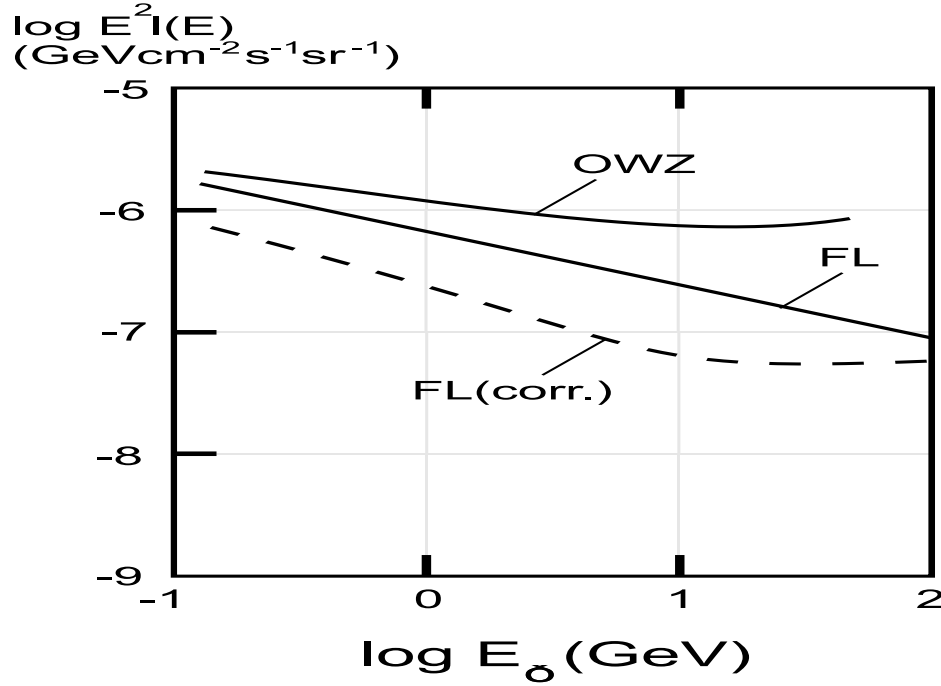


Figure 1: Comparison of the Fermi-LAT EG diffuse gamma ray spectrum [4], denoted FL with that derived earlier by us [13] and denoted ‘OWZ’. ‘FL(corr.)’ relates to the Fermi-LAT spectrum corrected for AGN.

at 100 EeV and to 14 Mpc at 1000 EeV. Corresponding values for Fe are: 3200 Mpc at 10 EeV, 630 Mpc at 100 EeV and about 2 Mpc at 1000 EeV. The results in [2] were for protons with an injection spectrum of E^{-2} and a maximum energy of 1000 EeV. The relative gamma ray intensities are given in Figure 2.

3.2 Sensitivity to the evolutionary model and other parameters.

In [2] we varied the (proton) injection spectrum with energy and maximum red-shift (z_m) using our earlier analysis as $G(E,z)dz = BE^{-\gamma}f(z) dz$, where $f(z) = H_0^{-1} (1+z)^{\beta-5/2}$ for $z < z_m$ and $f(z) = 0$ for $z > z_m$. H_0 is the Hubble constant.

Figure 3 (from [2]) gives the predicted spectra below 0.1 PeV for 3 variants of the parameters:

NC - no cosmological increase

C1 - $\beta = 3.7$, $z_m = 4$

C2 - $\beta = 3.7$, $z_m = 9$

In [2], C1 was regarded as the standard, ie for ‘normal galaxies’ an injection intensity varying as $(1+z)^{1.2}$ with $z_m = 4$ (this value approximating the redshift at which the volume density of active galactic nuclei begins to fall). The energy content: $1.3 \times 10^{-7} \text{ eV cm}^{-3}$ [2] is close to the value calculated from the assumption of an E^{-2} EG injection spectrum normalised to the contemporary measured spectrum [10] at 10 EeV.

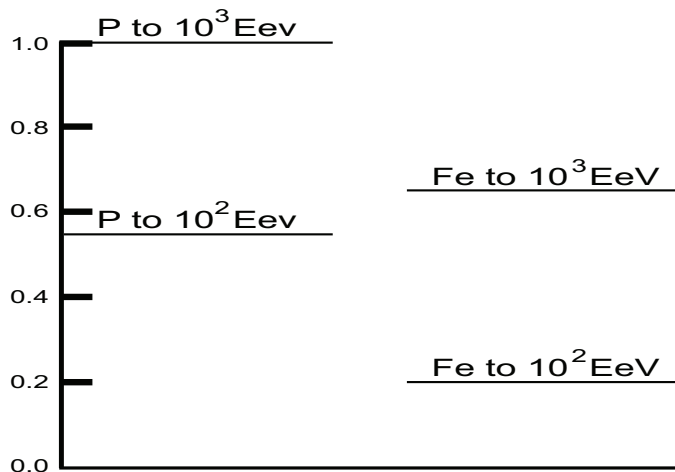


Figure 2: Contributions to the EG diffuse gamma ray intensity in the GeV region for two masses: protons and iron and two maximum injection energies: 10^2 and 10^3 EeV. Protons to a cut-off at 10^3 EeV' is taken as the datum. The ordinate is the relative contribution normalised to the standard of protons to 10^3 EeV.

Turning to the radiation fields, later work [14], has shown that the IR intensity is a factor 2 lower than assumed in [2]. However, the IR affects the ensuing gamma ray spectrum only above about 10^3 GeV and thus at higher energies than of interest here. The transition between Galactic and Extragalactic UHECR is still the subject of debate. Here we adopt 2 EeV as in all our previous and contemporary work. The use of a lower cut-off is not large because the initial gamma-particle interactions only start in the EeV region. What is important is the intensity and slope of the particle spectrum and another EG spectrum can easily be introduced into the calculations.

4 The maximum CR energy.

4.1 The analysis of EG gamma rays.

Inspection of figure 3 shows an anomaly in that the shaded region rises outside the expected range for $E_\gamma \lesssim 3$ GeV; this is a consequence of the observed gamma ray spectrum having a slope near -2.4, in comparison with the expected spectra having slopes near -2.0.

The reason for the discrepancy is probably the effect of CR electrons escaping from normal galaxies and interacting with the ambient radiation fields via the Inverse Compton effect. For such normal galaxies with an escaping electron flux above about 100 GeV having a slope -4.0, the eventual gamma ray spectrum would have slope ~ -2.5 , as required. Most of the electron-gamma rays would come from CR produced at high red shifts.

The contribution of the above from above 10 GeV would be expected to be small

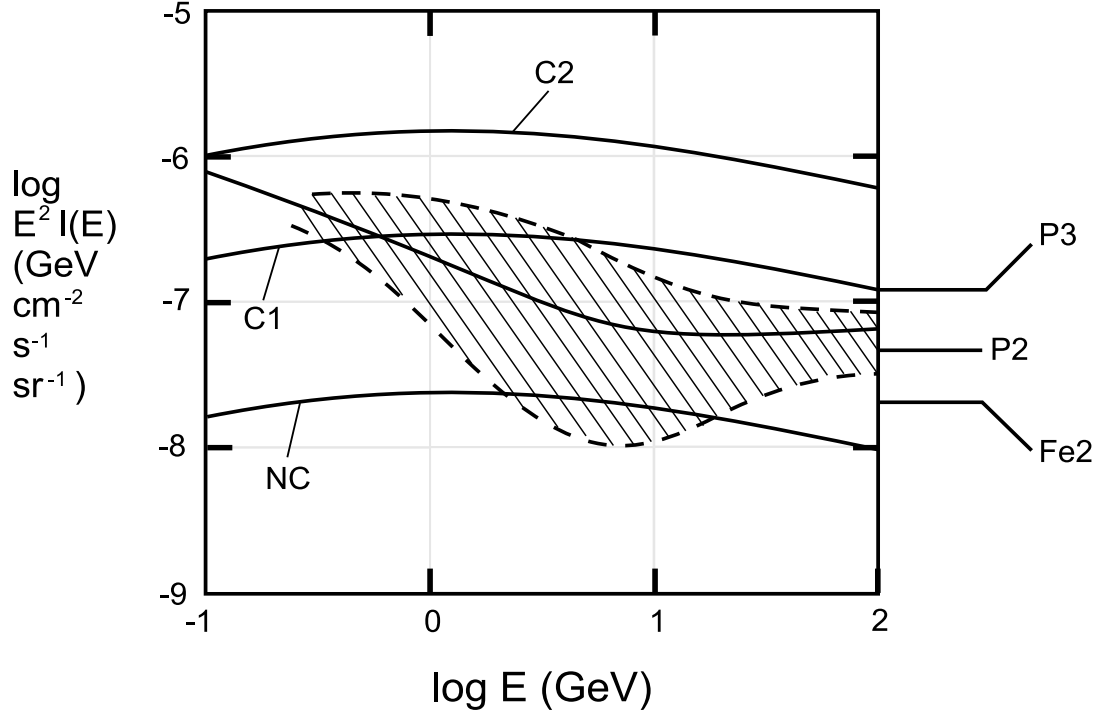


Figure 3: Comparison of the predicted EG diffuse gamma ray spectrum from [2] for:

NC, no cosmological increase in injection,

C1, the datum: injection as $(1+z)^{\beta-5/2}$, with $\beta = 3.7$ and $Z_m = 4$

C2, enhanced cosmological injection, with $\beta=3.7$ and $z_m = 9$.

The spectra are approximate. P2, P3 and Fe2 relate to the expected contributions from cascading from Figure 2. P2, P3 relate to protons with maximum energies 10^2 and 10^3 Eev, and Fe2 is for iron, limited to 10^2 Eev. The shaded area indicates the spread in estimates of the diffuse flux. In view of the many uncertainties in the values for the parameters (IG radiation fields, magnetic fields, primary CR spectra) the values for Fe2, P2 and P3 must be regarded as illustrative only.

because of the likely dearth of electrons of sufficiently high energies and thus we just adopt the gamma ray energy range in Figure 3 of 10 to 100 GeV.

The energy content available for the electromagnetic cascade is an obvious indicator of the particle charge, maximum energy combination, assuming, as usual, that the EG CR injection spectrum has a slope ~ -2 . Figure 3 shows the various possibilities normalised to the NC (p, 1000 Eev) results. (Note the proviso.)

Although the sensitivity of the flux to the combinations is not large (in terms of the spread in estimates of the diffuse flux - shown shaded) it is evident that predictions are in ‘the right region’. Specifically, taken literally, and using the results for E_γ : 10-100GeV, and following the PAO indications that the particles above 30 Eev are of ‘mixed composition’ [11,12], the results appear to indicate a maximum energy of about 100 Eev.

At this stage mention can be made of later work on this topic [16]. Understandably, the results are not identical, the differences being largely due to differences in essentially

all the values for the many relevant parameters: the intergalactic radiation fields and magnetic fields, the EG CR spectrum and its mass composition, the most likely form of the injection spectrum: its β and z_m values. The significance of these later results will be considered in §5.

4.2 The PAO results for Centaurus-A

There is rather strong evidence that some, at least, of the UHECR come from the nearest, very strong, radiogalaxy, Centaurus-A. Thus, PAO finds that about 24% of the particles can have come from this object, when allowance is made for the spread in arrival directions caused by the intergalactic and interstellar magnetic fields [10].

Figure 4 shows the PAO energy spectrum. Insofar as Cen-A is only some 2-3 Mpc away, the losses on the CMB are quite negligible and the true injection spectrum should be observed. With a slope of -2 the Cen-A spectrum should look as indicated. It is evident that the particles expected above 100 EeV are absent. Thus, this source of UHECR, at least, which would have been expected as a for-runner in the search for UHECR sources, does not emit particles above 100 EeV.

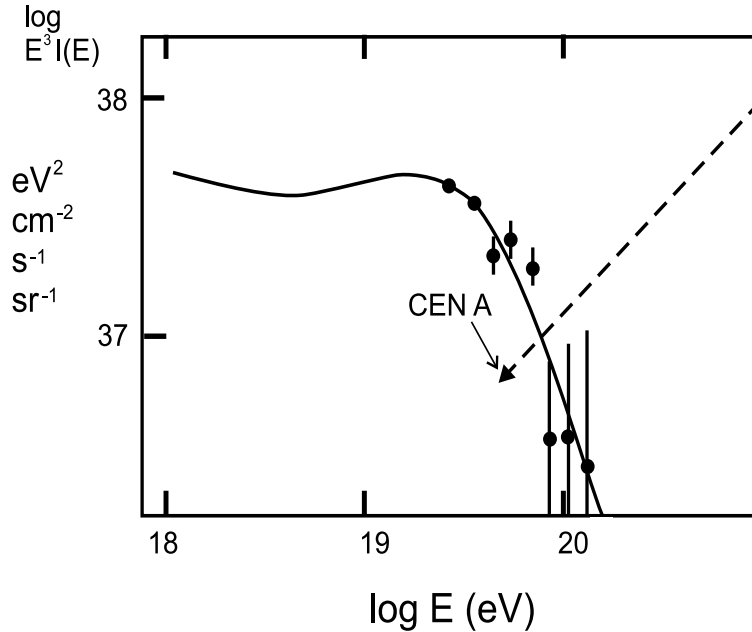


Figure 4: The PAO spectrum [10] and our estimate of what the Cen-A spectrum would look like if it were typical for the strongest EG sources and had spectral shape $\sim E^{-2.0}$ at injection and continued to 10^{21} eV. Insofar as the identification of Cen-A as the source of UHECR (4% probability of no effect [10]) the arguments are not (yet) firmly based.

4.3 Further work needed.

There are two other areas where further work is needed. The first concerns the measured UHECR spectrum from the PAO. This observatory is in the Southern Hemisphere and there is the possibility that the measured spectrum is not representative of the Global average. This follows from the likely non-uniform volume density of the sources over the Universe. That the volume density of ‘normal’ galaxies is not uniform has been known for some time. Recently, [17], the presence of a North-South anisotropy has been confirmed (at least for galaxies in the so-called N and S polar caps), the mean ratio of the N/S densities varying with distance, d , as: 4.3 locally, 3.5 at $d = 25$ Mpc, 1.6 at $d = 50$ Mpc, 1.23 at $d = 75$ Mpc, 1.33 at $d = 100$ Mpc and ~ 1.0 for $d: 100\text{-}300$ Mpc. Thus, if UHECR sources are distributed in the same way as ‘galaxies’ from the survey , there should be a difference between the UHECR intensities at such high energies where diffusion has not diluted the N-S anisotropy too seriously. It should be noted that the effect of a spectrum of primary masses will reduce the observed anisotropies if, as is likely, the anisotropy (amplitude and phase) is rigidity dependent.

It is interesting to note the increase in intensity of the EG component above 10^{19} eV with increasing energy for N with respect to S detectors [18], suggestive of the above hypothesis. It is possible that the well known N,S difference in apparent mass compositions above 10^{18} eV is also related to the N,S densities: the excess of nearby galaxies in the North will lead to an excess of light nuclei (He, CNO, but not protons) because of their short attenuation lengths. For example, for $E > 6 \cdot 10^{19}$ eV, the attenuation length is only 20 Mpc for CNO, whereas it is approaching 100 Mpc for protons and iron [18]. However, it is impossible to be dogmatic at this stage because the measured galaxy densities versus distance are only valid for restricted regions of the Universe and there is the ubiquitous problem of the effect of both Extragalactic and Galactic magnetic fields in smearing the arrival directions. The relevance of the above to the problem in hand is that there is still uncertainty in the effective average UHECR intensity, on a local cosmic scale, to use in the calculations and, correspondingly, the mass composition to take.

The second area relates to the values of the many parameters used in the calculations: β and z_m (Figure 3), the IG radiation and magnetic fields, the CR spectra and their masses and so on. An example is of z_m in the cosmological increase in CR injection efficiency. Recent work for AGN (eg [19]) suggests that it might be somewhat higher than the value of 4 adopted. If so, the constraint on the maximum CR energy could be more stringent.

5 More recent estimates of the EG gamma ray flux.

As mentioned earlier, recent analyses have been made [16] which are similar to ours [2] but using Fermi-LAT data for the observed gamma ray spectrum and adopting somewhat different values for some of the important parameters. For example, whereas we use an exponent 2.0 (the Fermi-value) for the true EG spectrum the workers in [16] use γ : 2.3 to 2.6. Another example in the value of z_{max} (see §3.2); we used $Z_m=4$, and justified it, whereas [16] adopted $z_{max} = 2$. The calculations in [16] were for protons

only, clearly at variance with the experimental situation [7, 8, 9].

The aim of [16] was to find the best-fit values of ‘n’ (related to our β) and the exponent of the EG spectrum, γ . The ‘HighRes’ spectrum [20] was used to derive the EG spectrum, with its required γ -value, to give a best-fit to the measured Fermi-LAT EG diffuse gamma ray spectrum. Comparison can be made via the derived energy content in the predicted gamma ray spectrum. Our value was $20 \cdot 10^{-6} \text{eVcm}^{-3}$, of values in the range 1-6 eVcm^{-3} in [16]. The difference in values between ourselves and [16] can be explained to within $\pm 30\%$ by the differences in γ , $n(\beta)$, input CR proton spectrum, etc.

What the computed energies do bring home is the sensitivity of the outcome (eg predictions of Figure 3) to the values for the parameters referred to, some of which are still poorly known. For example, changing the predictions by a factor 2 (not impossible) would change the conclusions considerably: for example, from P2 to Fe2.

6 Neutrino fluxes

The IceCube experiment [21] has recently observed high energy events indicative of the presence of neutrinos of energy in the PeV region: 2 events here and over 10 back to a TeV. It is interesting to note that back in the 1960s the KGF experiment [22] observed one such event - the ‘golden event’ of very high multiplicity. Such events are presumably due to neutrinos from the initial primary - CMB interaction at cosmological distances and the neutrinos, unlike the gamma rays, do not have a ‘threshold radius’. Other things being equal, the median distance of origin will be half the Hubble radius, i.e. of order 2000 Mpc compared with the gamma rays of main concern here which have a median distance of only 5-70 Mpc. In the calculations [eg 20] the assumption has been immediately made that the UHECR spectrum is uniform throughout the Universe (apart from its z -dependence). This need not be so. The discussion in §4.3 regarding the volume density of galaxies, which varies by at least ± 2 over the local 100 Mpc means that there is at least a further factor of ± 2 uncertainty in the predicted neutrino intensities, this is an addition to the uncertainty in the primary mass and maximum energy of the very distant UHECR.

The moral of the neutrino analysis is that differences of significance between observed and expected TeV to PeV intensities need not indicate exotic processes; more conventional differences need to be dismissed first.

7 Discussion and Conclusions

The very tentative result of the present work is that there is no evidence of UHECR being emitted from sources with energy above 100 EeV. More accurate estimates of the electron contribution to the EG diffuse gamma ray intensity are needed, as are further measurements of the UHECR spectrum and astronomical evidence for the spatial distribution of likely CR sources on 100 Mpc scales. Furthermore, values for the many parameters in the model need to be made. Indirect studies by way of high energy CR neutrino fluxes will also be of great value.

Acknowledgments

The authors are grateful to the Kohn Foundation for financial support.

References

1. Wdowczyk, J., et al., 1972, J.Phys. A. 5, 1419.
2. Wdowczyk, J. and Wolfendale, A.W., 1990, Astrophys. J. 349, 35.
3. Fichtel, C.E. et al., 1978, Astrophys.J., 222, 833.
4. Abdo, A. et al., 2010, Phys. Rev. Lett., 104, 101101.
5. Abazajian, K.N. et al., 2011, Phys. Rev. D 84,103007; arXiv:1012.1247.
6. Tkaczyk, W. et al., 1975, J.Phys.A. 8, 1518.
7. Wibig, T. and Wolfendale, A.W., 2009, Open Astron. Journ. 2, 95.
8. Abraham, J. et al., 2010, Phys. Rev. Lett., 104, 091101.
9. Watson, A.A., 2014, Rep. Progr. Phys., 77, 036901(24pp); arXiv:1310.0325
10. Abreu, P. et al. for the Pierre Auger Coll., 2010, Astropart. Phys., 34, 314; arXiv:1009.1855
11. Suchoy, O.B. et al., 2012, Adv. in Astron. and Space Phys. 2, 73.
12. Kim, H.B., 2013, J. Korean Phys. Soc. 62, 708.
13. Osborne, J.L. et al., 1994, J.Phys. G. 20, 1089.
14. Ord, M. et al., 2011, 32nd Int. Cosm. Ray Conf., Beijing, 8, 117.
15. Hooper, D. et al., 2007, Astropart. Phys., 27, 199; astro-ph/0608085.
16. Ahlers, M. et al., 2010, Astropart. Phys., 34, 106; arXiv:1005.2620
17. Whitbourn, J.R. and Shanks, T., 2013, Mon. Not. Roy. Astron. Soc.; arXiv:1307.4405.
18. Watson, A.A., 2013, IACTPP Villa Olmo Conf.:
[http : //villaolmo.mib.infn.it/presentations/IACTPP_2013](http://villaolmo.mib.infn.it/presentations/IACTPP_2013)
19. Fontanot, F, et al., 2012, Mon. Not. Roy. Astron. Soc. 425, 1413.

20. Aartsen, M.G. et al., 2013, Phys. Rev. Lett., 111, 021103;
2013, Science, 342, 1242856; arXiv:1304.5356; arXiv:1311.5238.
21. Ahlers, M. and Halzen, F., 2012, arXiv:1208.4181.
22. Achar, C.V. et al., 1965, Proc.9th Int. Cosm. Ray Conf., London,
2, 1012.